Nuclear Materials and Energy 37 (2023) 101506

Contents lists available at ScienceDirect

Nuclear Materials and Energy

journal homepage: www.elsevier.com/locate/nme

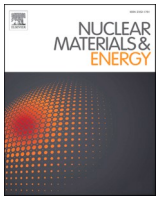

Tungsten based divertor development for Wendelstein 7-X

Joris Fellinger [a], M. Richou [b], G. Ehrke [a], M. Endler [a], F. Kunkel [a], D. Naujoks [a], Th. Kremeyer [a], A. Menzel-Barbara [a], Th. Sieber [a], J-F. Lobsien [a], R. Neu [c], J. Tretter [c], Z. Wang [c], J-H. You [c], H. Greuner [c], K. Hunger [c], P. Junghanns [c], O. Schneider [c], M. Wirtz [d], Th. Loewenhoff [d], A. Houben [d], A. Litnovsky [d], P-E. Fraysinnes [h], P. Emonot [h], S. Roccella [f], O. Widlund [e], B. Končar [g], M. Tekavčič [g], the W7-X team [1]

[a] Max Planck Institute for Plasma Physics, 17491 Greifswald, Germany
[b] CEA Institute for Magnetic Fusion Research (IRFM), 13108 St Paul-lez-Durance Cedex, France
[c] Max Planck Institute for Plasma Physics, 85748 Garching, Germany
[d] Forschungszentrum Jülich GmbH, Institut für Energie- und Klimaforschung – Plasmaphysik, 52425 Jülich, Germany
[h] CEA, LITEN, DTCH, LCA, F-38000 Grenoble, France
[f] ENEA – Frascati Research Centre, 00044 Frascati, Italy
[e] RISE Research Institutes of Sweden, 400 22 Göteborg, Sweden
[g] Jožef Stefan Institute, 1000 Ljubljana, Slovenia

ARTICLE INFO

Keywords:
Wendelstein 7-X
Divertor
High heat flux
Additive manufacturing
Diffusion welding
Hot isostatic pressing
Galvanization
Plasma spraying
Tungsten
WNiFe
CuCrZr

ABSTRACT

Wendelstein 7-X, the world's largest superconducting stellarator in Greifswald (Germany), started plasma experiments with a water-cooled plasma-facing wall in 2022, allowing for long pulse operation. In parallel, a project was launched in 2021 to develop a W based divertor, replacing the current CFC divertor, to demonstrate plasma performance of a stellarator with a reactor relevant plasma facing materials with low tritium retention. The project consists of two tasks: Based on experience from the previous experimental campaigns and improved physics modelling, the geometry of the plasma-facing surface of the divertor and baffles is optimized to prevent overloads and to improve exhaust. In parallel, the manufacturing technology for a W based target module is qualified.

This paper gives a status update of project. It focusses on the conceptual design of a W based target module, the manufacturing technology and its qualification, which is conducted in the framework of the EUROfusion funded WPDIV program. A flat tile design in which a target module is made of a single target element is pursued. The technology must allow for moderate curvatures of the plasma-facing surface to follow the magnetic field lines. The target element is designed for steady state heat loads of 10 MW/m^2 (as for the CFC divertor). Target modules of a similar size and weight as for the CFC divertor are assumed (approx. < 0.25 m^2 and < 60 kg) using the existing water cooling infrastructure providing 5 l/s and roughly maximum 15 bar pressure drop per module.

The main technology under qualification is based on a CuCrZr heat sink made either by additive manufacturing using laser powder bed fusion (LPBF) or by uniaxial diffusion welding of pre-machined forged CuCrZr plates. After heat treatment, the plasma-facing side of the heat sink is covered by W or if feasible by the more ductile WNiFe, preferably by coating or alternatively by hot isostatic pressing W based tiles with a soft OFE-Cu interlayer. Last step is a final machining of the plasma-exposed surface and the interfaces to the water supply lines and supports to correct manufacturing deformations.

1. Introduction

Wendelstein 7-X (W7-X), the largest modular stellarator in the world with a plasma volume of 30 m^3, is a tenfold symmetric device. Seven different superconducting coil types enable a large magnetic configuration space. Long pulse operation started in 2022 after exchange of the uncooled graphite test divertor units (TDU) with water-cooled divertor units with a carbon fiber carbon (CFC) surface, see Fig. 1. Both divertors have the identical plasma facing surface geometry. The divertor intersects the magnetic islands, which isolate the divertor

[1] Full list of team members available in [1].

https://doi.org/10.1016/j.nme.2023.101506
Received 28 June 2023; Received in revised form 29 August 2023; Accepted 8 September 2023
Available online 9 September 2023

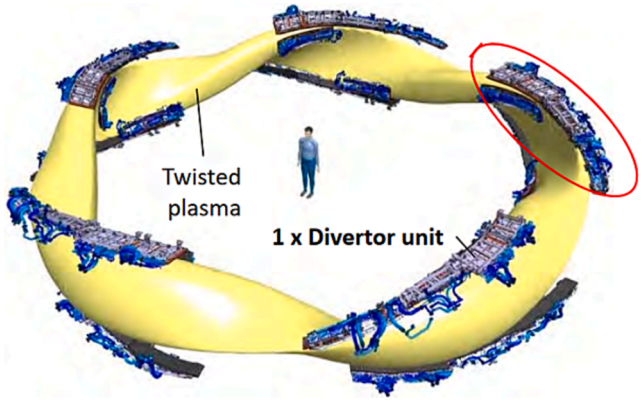

Fig. 1. Plasma of W7-X with ten water-cooled divertor units.

from the core. The baffles are positioned as close as possible to the islands to maximize plugging of neutrals generated at the strike lines on the divertor, see Fig. 2.

An important next step of the roadmap towards a reactor based on the stellarator concept is the demonstration of high performance plasmas in W7-X with a tritium compatible plasma-facing surface despite the expected bigger impact of impurities from W compared to those from the current CFC surface.

For that purpose, a project team was formed in 2021 assessing the best strategy to upgrade the plasma facing components (PFCs) to a carbon free device. It was decided to develop a new divertor and new baffles with a pure tungsten (W) or W-based plasma-facing surface. Making a new design allows for changes to the geometry to include lessons learnt from manufacturing, installation and operation. Graphite tiles on other PFCs will be either W-coated or gradually be replaced by W-based tiles [1].

This paper gives a status update of the ongoing R&D activities of the new divertor design.

In the next section, lessons learnt from manufacturing, installation and plasma operation of the CFC divertor and baffles will be discussed as well as the requirements to the new design. The modification of the plasma-facing geometry is primarily based on results of edge plasma modelling whereas the modification of the component design focusses on simplification of the manufacturing and inspection process and mainly requires qualification of technologies. Section 3 gives an overview of the tool development to speed up the exchange between CAD and physics based models for magnetic fields and plasma behavior. A simplified concept of the target module is proposed in section 4, supported by simulations showing the compatibility with W7-X loading conditions. Section 5 shows the progress of qualification of key technologies. Finally, an outlook for the completion of the project is given in section 6.

As an alternative to a complete new design, it is worth noticing that investigations led by Forschungzentrum Jülich are ongoing in parallel to make an in-situ W-based coating on the existing plasma facing components [2]. Obvious advantages of this solution are the potential time and cost savings compared to a new design, but operational limitations caused by the geometry of the current divertor cannot be resolved.

2. Lessons learnt

2.1. From manufacturing CFC target modules

The divertor unit consists of three vertical and nine horizontal target modules intersecting the strike lines and sided by nine and eight baffle modules at inboard and outboard side respectively, see Fig. 2. The highly loaded CFC target modules are made of eight to twelve target elements (TEs) with 50–61.5 mm width and 250–595 mm length [3,4,5]. Each TE consist of a CuCrZr heat sink, which is made of two E-beam welded plates and protected against the plasma with carbon fiber reinforced carbon (CFC) tiles of 6–8 mm thickness. A 0.4 mm thin copper layer is cast onto the CFC tiles by active metal casting (AMC) and then a 2.6 mm soft oxygen-free electronic (OFE) copper interlayer is bonded to the AMC copper by hot isostatic pressing (HIP). Next, the tiles are e-beam welded onto the heat sink and finally the plasma-facing surface is machined to the desired shape. In the straight parts of the cooling channel, a swirl tape is included to enhance the turbulence and heat removal capability of the heat sink. After machining the CFC, the TEs are mounted on a steel structure with 0.1 mm step tolerance between them at the plasma-facing side to limit leading edges. Finally, the TEs were welded to stainless steel pipes by e-beam welding using a Ni transition part between the CuCrZr and stainless steel.

Welding was a very tedious work as weld distortion tended to destroy the step tolerance and some leaks were detected at the Ni adapter that was therefore strengthened and sealed with a galvanic copper coating of 0.3 mm [6]. In initial high heat flux (HHF) tests, some TEs failed due to

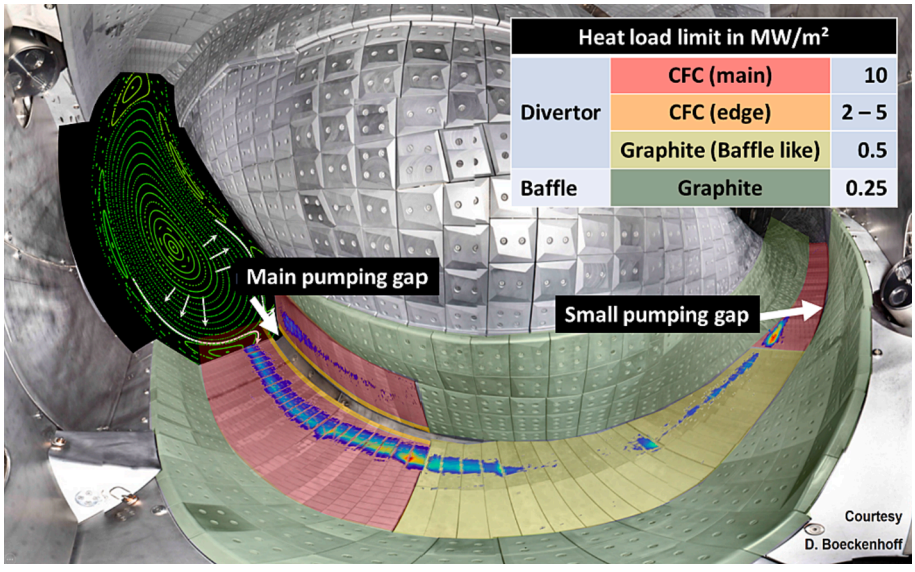

Fig. 2. Plasma facing components with the heat load limits of the CFC divertor and an exemplary overlay of a Poincare plot of the magnetic field and a heat load pattern.

delamination at the outer contour of the CFC-Cu interface, see Fig. 3. It is attributed to delamination stresses resulting from thermal expansion mismatch, which is approximately proportional to the attained temperature at the interface [7]. Since the front and top end tile (see Fig. 3) suffer from reduced cooling at the U-turn of the cooling channel, their allowed heat load was reduced to 2 and 5 MW/m^2 respectively.

Overall, the target element production was a very cumbersome task including 82 manufacturing and 44 inspection steps [3]. The clear ambition for the new divertor is to reduce the number of manufacturing and inspection steps, specifically by reducing the number of weld seams. To allow for a strike line close to the pumping gap, it is pursued to increase the allowed heat load of the front and top end tile to 10 MW/m^2.

2.2. From installation

Installation of the divertor and baffle modules in the plasma vessel was extremely challenging for several reasons:

- The modules with a high weight up to ~80 kg could only be brought into the vessel by hand and they were positioned either by hand or in combination with a dedicated positioning tool.
- The tight and irregular space of the vessel provides hardly any space for maneuver of personnel.
- Target and baffle modules had to be installed in the plasma vessel in a dedicated order to ensure access to weld the connections to the pre-installed cooling water supply lines.
- Due to a lack of space, flexible hoses were not feasible for all supply lines, thus requiring an exact fitting between rigid pipes and rigid target module to make the final leak tight connection.
- An installation tolerance of 0.2 mm was required to minimize leading edges between modules.
- Tight damage tolerances on sensitive CFC surface required a very careful installation and elaborate protection measures.
- The support system of the divertor modules was statically indeterminate. As a result, tightening of the support bolts induces deformations in the modules and the position of the modules depends on the tightening forces. This made positioning of the modules within the required accuracy a very tedious task.
- In some modules additional diagnostic systems had to be integrated like the pre-installed divertor gas injection system with sensitive nozzles and pop-up Langmuir probes.

To relax the installation issues, it is essential to reduce the weight as much as possible despite the fact that an exchange of 7 mm CFC to 3 mm W causes a ~10 kg increase for a 0.25 m^2 module. Furthermore, the water supply lines in the vessel should not be changed as de- and re-installation from the inboard side of the vessel is no longer feasible without substantial de-installation of many ex-vessel components.

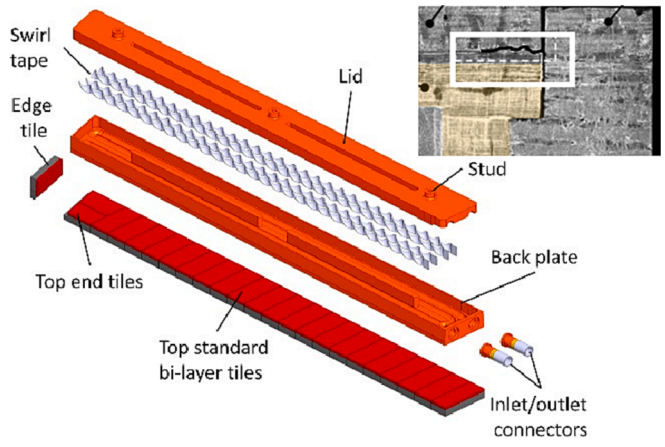

Fig. 3. Exploded view of a TE (left) [3] and delamination crack at the CFC-Cu interface of the top end tile (right) [8].

2.3. From experiments

Experiments with the TDU successfully confirmed the reduced neoclassical transport optimization of W7-X. The divertor is working well, allowing for stable and complete detachment [9]. Moreover, heat loads patterns and intensities are generally in good agreement with model predictions and they are projected to remain below the design value of 10 MW/m^2 of the water-cooled divertor at planned input power of 10 MW [10]. However, there are some noticeable deviations [11], causing overloads on baffles and the baffle like middle part of the divertor, which reduce the freedom of operation. To generate more operational freedom, an allowed heat load of the baffles and middle part of the divertor of 1 and 10 MW/m^2 respectively is aspired.

The ratio of the neutral pressure at the divertor to the main chamber is generally low [10,12] and the efficiency of the small pumping gap is significantly better than that of the main pumping gap [13] indicating that neutrals entering the main pumping gap are mainly returning back into the plasma volume. To improve pumping of neutrals, it is pursued to bring the strike line as close as possible to the pumping gap and to modify the shape of the plasma-facing surface and pumping gap panels to reflect the neutrals in the direction of the pump.

Although impurity confinement times were small in the campaigns so far, impurity accumulation could be a challenge for long pulse high performance discharges [14]. Obviously, the impurity challenge becomes even bigger for W-based plasma-facing surfaces. W-particles are feared to have a tendency for enrichment and accumulation in the core resulting in significant stronger radiation losses compared to carbon.

3. Coupling of physics based models with CAD

EMC3-lite [15] and EMC3-Eirene [16] are the working horse modelling tools for the prediction of heat loads and neutral particle physics in the edge plasma [17]. For the optimization of the plasma-facing geometry with respect to multiple goals like particle exhaust, heat loads and impurity control, tools are under development to facilitate the exchange between CAD and EMC3-lite (and EMC3-Eirene). Moreover, the existing plasma-facing geometry was simplified and parametrized in CAD to allow for rapid modification.

In the order to obtain a CAD geometry of the volume of high heat fluxes in the edge plasma, which are carried mainly in the outermost flux surface of the magnetic islands, a tool was developed to create the CAD shape of the islands for any magnetic configuration including effects from plasma currents. Field lines are traced with the Extender based on consistent equilibrium simulations by VMEC [18] and then Fourier transformed in magnetic coordinates. The description of the surface with Fourier components can be transformed by standard python library into a STP-file. The intersection between this flux surface and the divertor is a prerequisite to get a strike line and allows for a quick scan of incident angles and unintended intersections with for instance the baffles (see Fig. 4). Whether strike lines actually pop up at the intersection depends obviously on shielding by other divertor components.

Another tool is being developed to find the optimal subdivision of the plasma-facing geometry in target modules with respect to leading edges and ease of installation. Based on a database of FEM simulations with temperature fields of target elements for various heat loads, incident angles and leading edges, a tolerable leading edge not exceeding material temperature limits can be interpolated for any combination of heat load and incident angle. Combining this result with EMC3-Lite simulations of heat load patterns, the allowed leading edge size is calculated for the entire plasma-facing surface for a range of magnetic configurations. It shows that while for some areas of the plasma-facing surface, no leading edges of more than 0.1 mm can be tolerated, large areas can accept leading edges up to 1 mm. Combining this data with the

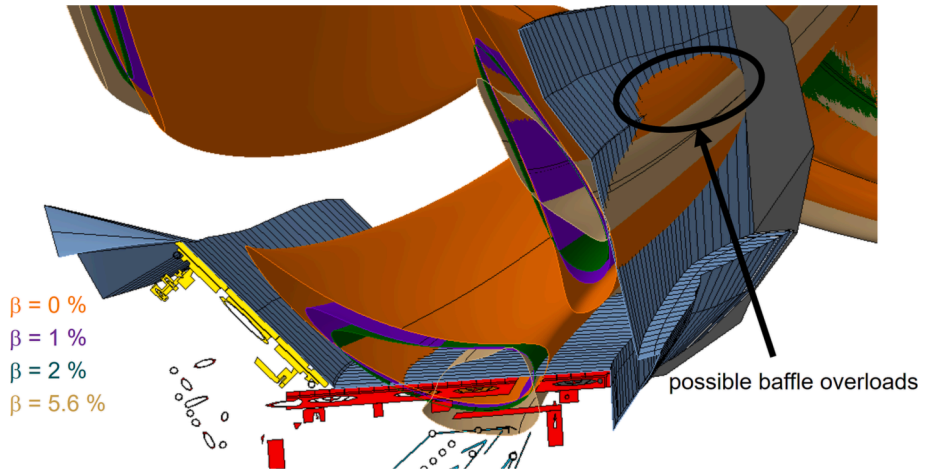

Fig. 4. CAD geometry of outermost flux surface of the islands in standard configuration for β values (ratio of plasma pressure to the magnetic pressure) between 0 % and 5.6 %.

clockwise or counterclockwise direction of the incident heat flux per magnetic configuration, critical areas are identified, where shielding is not possible and stringent step tolerances must be kept. Notably, to accommodate for thermal expansion, a nominal gap of 5 mm is foreseen between target modules, which inevitably causes a leading edge. In avoiding these critical areas as target module boundary, position tolerances for target module installation can be relaxed.

4. Conceptual design

4.1. Design objectives

A concept design for a new target module was developed using following subjective goals:

- The new plasma-facing surface geometry will be similar in size and flatness to the existing CFC divertor, even though it has not been defined in detail.
- The existing infrastructure for water-cooling will be used. It provides 12 supply lines of 5 l/s each at an allowable pressure drop of 15 bar. Consequently, the new target surface is assumed to be split into 12 target modules, each connected to one supply line.
- The allowed heat load capacity of the divertor is 10 MW/m^2 over a poloidal width of 100 mm. This value should also apply for the top end and front tile near the pumping gap if feasible.
- The target module weight should be minimized to preferably <60 kg.
- The number of manufacturing and inspection steps should be minimized.

Based on these objectives, a target module made of a single target element was developed, in which the manifold is integrated (see Fig. 5).

4.2. Design features

The concept design has following features:

- The plasma-facing surface is made of W or WNiFe. Based on the experience from ASDEX Upgrade [19], WNiFe is a very attractive candidate as plasma-facing material as this material shows acceptable sputtering under HHF. Moreover, it is isotropic, it is easier to machine and has substantial higher ductility than pure W. WNiFe is a 2-phase material of predominantly W grains in a NiFe matrix in which up to ~10 % W atoms are dissolved [20]. In ASDEX Upgrade W_{97}NiFe was used, whereas for W7-X W_{95}NiFe is chosen since it has further improved ductility [20]. The WNiFe is slightly magnetic [19] but it has been calculated that the resulting field errors in W7-X are acceptable.
- A bolted contact between the W-based plasma-facing material and the CuCrZr based heat sink is only feasible at moderate heat loads up to ~1 MW/m^2. For instance, the graphite foil used to enhance the thermal conductance between graphite and heat sink in the existing baffle design has a thermal conductance of ~2 kW/m^{2}K, which yields a ~500 K temperature jump at 1 MW/m^2 in steady state. With a maximum CuCrZr temperature of ~450 °C, a W temperature of 950 °C would occur at the interface, which is acceptable. At 10 MW/m^2 a temperature jump of 5000 K would occur, which is not tolerable. Therefore, a continuous bond between W and Cu based materials is needed, at the expense of thermal stresses due to the thermal expansion mismatch. This mismatch induces a strain singularity resulting in local peak delamination stresses along the boundary of the interface [22].
- To moderate the peak stresses a 1 mm soft OFE-Cu interlayer is applied between the W based material and CuCrZr based heat sink. At 10 MW/m^2 only a temperature gradient of ~25 K occurs over such interlayer in steady state.

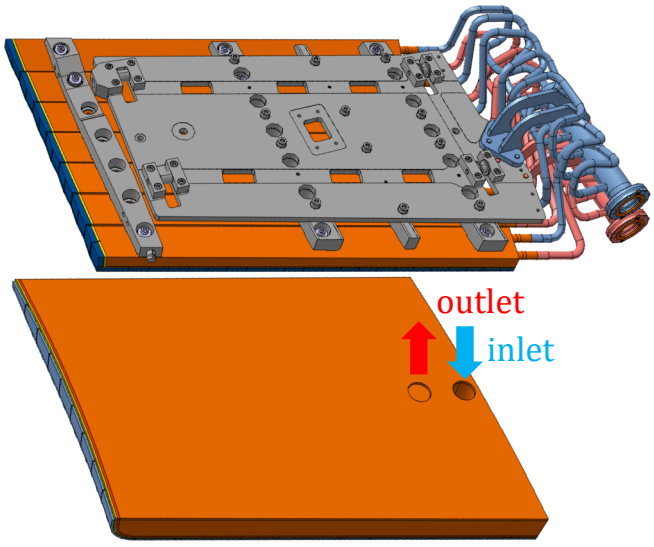

Fig. 5. Replacement of target module 1 h (top) with seven TEs, a steel support structure, 14 flexible pipes and two manifolds by one single TE module (bottom).

- The thermal stress at the W-Cu interface is in first order proportional to the attained temperature range at the interface. To minimize this range, the interface must be as close as possible to the water cooling channel.
- To minimize the thermal stress and the degradation of mechanical properties, the heat removal capacity being the product of the transfer coefficient (HTC) along the water-cooling channel and the cooling channel surface area must be maximized. Since the HTC is in first order proportional to the water velocity v (e.g. Gnielinski correlation), and the pressure drop to v^2 (e.g. Darcy–Weisbach equation), the heat removal capacity is constrained by the allowed pressure drop and available mass flow rate. To remain within the pressure drop budget, the velocity may only be maximized in areas where heat is actually removed, and it must be minimized in areas where no heat is removed. In regions of high velocity, bends in the channel must be minimized. Along these lines, the U-turn of the water channel near the pumping gap contains a high flow speed region of 90° along the plasma facing surface with largest possible bending radius (~30 mm), limited by the thickness of the heat sink, and a low flow speed region at the cold side with smaller bending radius.
- In order to keep the W-Cu interface in this region as close as possible to the water channel, the plasma facing surface follows the contour of the channel.
- To minimize the deformation of the single TE module, the cold part of the heat sink (which exhibits no thermal expansion during operation) must be stiff compared to the hot part of the heat sink including the W based tiles and OFE-Cu interlayer (exhibiting a thermal gradient causing bending). In doing so, the overall deformation is dominated by the stiff cold part.
- By using the stiff cold side of the heat sink for the return of the water, a return channel with large cross section with corresponding low flow speed and pressure drop is achieved (see Fig. 6).

4.3. Design analyses

To demonstrate the capability of conceptual target module design of Fig. 6, thermal–mechanical calculations and Lorentz fore calculations have been carried out.

The material properties are based on ITER Material Properties Handbook for OFE-Cu and CuCrZr, thermal properties of WNiFe from [19], and a simplified pure elastic assumption for WNiFe. The thermal model assumes a HTC at the cooling channel surface of 20 kW/m^{2}K, which is conservative according to the Gnielinski correlation for the flow speed in the narrow channels of 6.6 m/s. A CFD analyses of the actual HTC and pressure drop is pending.

FEM analyses show that the temperature even at the curved tile remains below 400 and 800 °C for CuCrZr and WNiFe respectively, under 10 MW/m^2 steady state load.

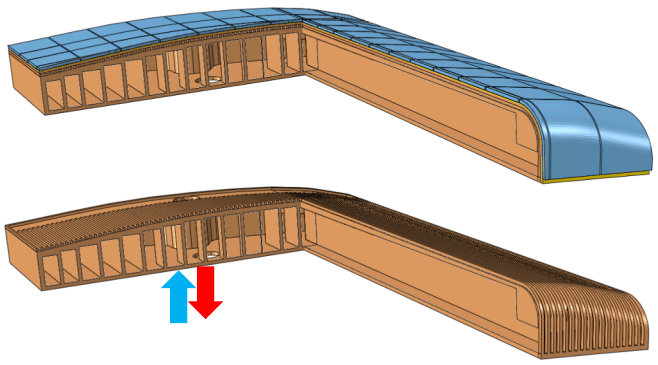

Fig. 6. Cross sectional view of the single TE module (top) and of cold part of the heat sink (bottom).

The corresponding deformation based on elastic–plastic analyses is<3 mm normal to the plasma-facing surface (compared to 5 mm for the CFC divertor) even though a cantilevered support system at the inlet and outlet was conservatively assumed (see Fig. 7).

Eddy currents due to a superconducting coil discharge or a plasma decay and corresponding Lorentz forces are proportional to the change of the enclosed magnetic flux and the thickness t of the conducting component. Since bending stiffness is proportional to t^3, thin structures are more critical than massive structures. As a heat sink of the size of a target module encloses significantly more magnetic flux than the ~60 mm wide heat sinks of the CFC divertor design, the Lorentz forces induced in the new design were analyzed for two cases: a superconducting coil discharge in 3 s (45 cases for the entire magnetic configuration space) and a plasma decay in 1 ms (21 cases with β up to 5.6 % and a toroidal current of 50 kA). The magnetic flux passing perpendicular through the target and baffle modules modelled as a copper plate was calculated using VMEC and Extender [18]. The maximum perpendicular magnetic field component is ~20 mT (see Fig. 8) and attributed to the toroidal and Pfirsch-Schlüter currents. The diamagnetic current, however, does not directly contribute to this flux as this torus-shaped closed current loop is only generating a toroidal field inside the plasma, which is roughly 50 mT at a diamagnetic energy of 5 MJ. Nevertheless, once this current decays, a current immediately rises in the plasma vessel, keeping the integral toroidal flux inside the vessel upright. As the cross section of the vessel is ~2.5x larger than that of the plasma, the change of the magnetic field experienced by the PFCs is ~20 mT. The incident angle of the field onto the PFC surface is typically below 6° (with the aim to limit heat loads) resulting in a change in the perpendicular magnetic field component below 2 mT. The maximum induced current over all modules due to the combined effect of all plasma currents is limited to 6 kA and forces on supports are<6 kN, which is not critical.

In addition, to prevent sharing of eddy currents from the stainless steel plasma vessel by the better conducting copper target and baffle modules, the connections of the modules to the vessel must be electrically isolated.

4.4. Manufacturing technologies

The CuCrZr heat sink can be made either by additive manufacturing, i.e. laser powder bed fusion (LPBF) or by diffusion welding plates in which the cooling channels are machined before joining them. Additive manufacturing provides great geometrical design freedom and an automated and thus controlled process. A heat treatment after manufacturing is needed to obtain acceptable mechanical and thermal properties [23]. If needed, the heat treatment could be integrated with a hot isostatic pressing cycle, to reach a leak tight maximum density without substantial changes to the microstructure. Diffusion welding has the advantage that the base material is not melted. Compared to brazing,

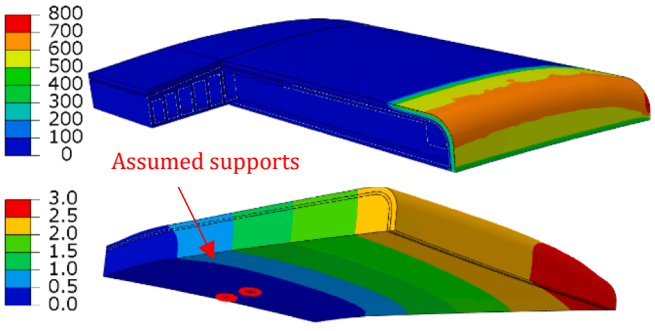

Fig. 7. Temperature [°C] at curved edge tile at 10 MW/m^2 steady state heat load (top) and displacement [mm] for most unfavorable strike line position (bottom).

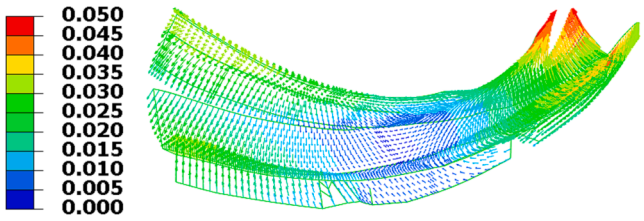

Fig. 8. Magnetic field [T] on divertor and baffle modules due to plasma currents in standard configuration with β of 5.6 %.

no new constituents are introduced at the interface, which otherwise might cause undesired effects on the mechanical or physical properties during operational cycles.

As deformations during manufacturing occur, the heat sink is machined to the plasma facing shape afterwards (if needed) and leak tested.

To cover the heat sink with W or WNiFe at the plasma facing side, preferably, the W based plasma facing material is coated onto the heat sink by low pressure plasma spraying (LPPS) [2] or radio-frequency inductively-coupled plasma spraying (RFPS) [24]. Based on expected erosion rates in W7-X a minimum thickness of 0.2 mm for the exposure time of ~300 h during the lifetime of W7-X is required, assuming an erosion rate of 0.2 nm/s [25]. To add additional safety, a minimum coating thickness of 0.5 mm is pursued.

Before coating, first the soft OFE-Cu interlayer is galvanized onto the heat sink. Also functionally graded coatings (W and stainless steel of 1–1.5 mm thickness) have been successfully demonstrated on laboratory scale surviving 1000 heat cycles up to 800 °C [26]. It is planned to evaluate if a graded coated mixture of W or WNiFe with OFE-Cu onto CuCrZr is also feasible. In that case the galvanized interlayer could be avoided, thus reducing the number of manufacturing steps.

It must be noted however, that a high heat flux performance of a full scale W based coating onto CuCrZr heat sink has not yet been demonstrated.

Therefore, alternative to coating, W based tiles can be joint to the heat sink by hot isostatic pressing (HIP). In this case, the OFE-Cu interlayer is first joint to the W based tile by casting, galvanization or diffusion welding. The plasma facing side of the heat sink must be machined to allow an accurate placing of a mosaic of these tiles. In a final step the tiles are joint by HIP to the heat sink at moderate temperatures (~500 °C) to avoid overaging of the CuCrZr. Due to cool down in the final HIP process, substantial thermal deformations occur which according to FEM analyses can be reduced by using a mosaic of tiles of approximately 40x40 mm rather than a continuous W-based cover. The slits between the tiles must be deep enough however to avoid sputtering of copper during plasma operation, i.e. a tile thickness of ~3 mm is required.

As a last step, the plasma-facing surface and the interfaces to the water-cooling supply lines and support system are machined to their final shape. For the W-based material wire erosion is the preferred technology, since it does not exert large forces which could harm the soft OFE-Cu interlayer otherwise.

5. Technology qualification

The qualification concentrates on technologies that are essential for the manufacturing of the conceptual design of the target module as described in the previous section.

First results on additive manufacturing carried out by Fraunhofer IGCV (see Fig. 9) show that a density greater than 99.7 % can be reached on small scale samples. Also, turbulence promoting swirls in the cooling channels can be integrated in manufacturing. The perfect thermal contact between swirl and heat sink allows the swirl to contribute to heat removal as well. Pipe samples with wall thicknesses between 1 and 3 mm were leak tight before heat treatment (tested at 20 °C and 40 bar, with requirement He leak rate $< 1 \bullet 10^{-9}$ mbar•l/s) but after heat treatment some samples did not pass the test. This will be investigated further.

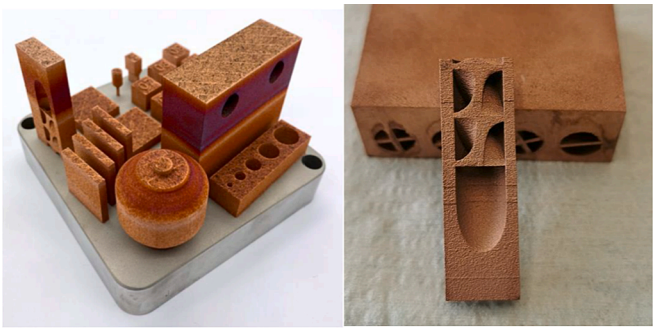

Fig. 9. Examples of LBPF manufactured CuCrZr samples (left) and a part of a heat sink containing a Ø 9 mm swirl (right).

First results reached by Steinbeis Tranferzentrum show that CuCrZr can be diffusion welded to CuCrZr without pores, see scanning electron microscopy (SEM) images in Fig. 10. Surfaces, which are to be welded, must be scratch free. Pressure and temperature history during welding can be optimized Higher pressures and temperatures allow for larger initial tolerances at the expense of larger residual deformations and larger gain sizes after welding.

Machining the plasma-facing surface to the final shape with wire erosion shows that WNiFe is much easier to machine than pure W. After wire erosion a cleaning of the surface is mandatory as the surface gets contaminated with brass of the wire.

6. Summary and outlook

A project was established to develop a W-based divertor including baffles. Tools are under construction to easily exchange data between physics based models and CAD geometries to speed up optimization of the plasma facing geometry with respect to heat loads, impurity transport and particle exhaust. In parallel, with the aim to simplify manufacturing and inspection as much as possible, a concept for a target module has been established based on a single target element covered with W95NiFe. Modern manufacturing technologies like diffusion welding, additive manufacturing, plasma spraying of W-based coatings and HIP of tiles onto heat sinks are under qualification. First results from diffusion welding and additive manufacturing show that these technologies could be suitable for manufacturing CuCrZr heat sinks.

For the next few years, qualification will be pursued from small-scale samples up to full mock ups, to be tested in HHF tests. Once the new plasma facing geometry is defined, a detailed design for all modules is foreseen including a detailed planning of budget and schedule, which will be the basis of a go/no-go decision of a complete replacement of the current CFC divertor. Alternatively, a gradual replacement of those modules that limit operation like the baffle-like divertor modules (see Fig. 2), could enlarge the experience in manufacturing and installation of W-based modules before taking the final go/no-go decision.

CRediT authorship contribution statement

Joris Fellinger: Conceptualization, Methodology, Investigation, Visualization, Writing – original draft. **M. Richou:** Supervision, Writing – review & editing. **G. Ehrke:** Investigation. **M. Endler:** Validation. **F. Kunkel:** . **D. Naujoks:** Conceptualization. **Th. Kremeyer:** Conceptualization. **A. Menzel:** Investigation. **Th. Sieber:** Resources. **J-F. Lobsien:** Resources. **R. Neu:** Supervision, Funding acquisition. **J. Tretter:** Resources. **Z. Wang:** Investigation. **J-H. You:** Conceptualization. **H. Greuner:** Resources. **K. Hunger:** Investigation. **P. Junghanns:**

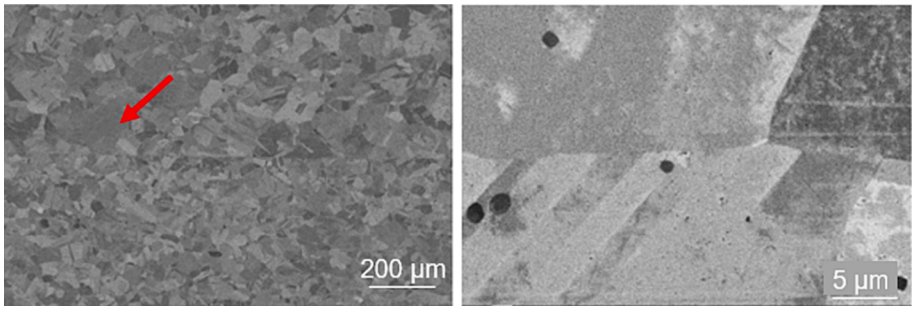

Fig. 10. SEM image of diffusion welded CuCrZr samples.

Investigation. **O. Schneider:** Project administration. **M. Wirtz:** Resources. **Th. Loewenhoff:** Resources. **A. Houben:** Investigation. **A. Litnovsky:** Conceptualization. **P-E. Fraysinnes:** Conceptualization. **P. Emonot:** Conceptualization. **S. Roccella:** Resources. **O. Widlund:** Resources. **B. Končar:** Investigation. **M. Tekavčič:** Investigation.

Declaration of Competing Interest

The authors declare that they have no known competing financial interests or personal relationships that could have appeared to influence the work reported in this paper.

Data availability

Data will be made available on request.

Acknowledgements

This work has been carried out within the framework of the EUROfusion Consortium, funded by the European Union via the Euratom Research and Training Programme (Grant Agreement No 101052200 — EUROfusion). Views and opinions expressed are however those of the author(s) only and do not necessarily reflect those of the European Union or the European Commission. Neither the European Union nor the European Commission can be held responsible for them

References

[1] Naujoks et al., Nuclear Materials and Energy, this issue, to be published (JNME-D-23-00136), 2023.
[2] Keller, et al., Metals 13 (2023) 531.
[3] Boscary et al. (2017), Fusion Engineering and Design 124.
[4] Boscary et al., in: IEEE 25th Symposium on Fusion Engineering (SOFE), 2013.
[5] Boscary, et al., Fusion Eng. Des. (2009) 84.
[6] Junghanns, et al., Fusion Eng. Des. 124 (2017).
[7] You, et al., Fusion Eng. Des. (1998) 38.
[8] Boscary, et al., Fusion Eng. Des. (2012) 87.
[9] S. Pedersen, et al., Nuclear Fusion 62 (2022), 042022.
[10] S. Pedersen, et al., Nuclear Fusion 59 (2019), 096014.
[11] Gao, et al., Nuclear Fusion 60 (2020), 096012.
[12] Kremeyer, et al., Nuclear Fusion 62 (2022), 036023.
[13] Haak, et al., Plasma Phys. Control. Fusion 65 (2023), 055024.
[14] Langenberg, et al., Nuclear Fusion 61 (2021), 116018.
[15] Gao, et al., Nuclear Fusion 63 (2023), 026031.
[16] Feng, et al., Plasma Phys. Control. Fusion 64 (2022), 125012.
[17] Feng, et al., Contrib. Plasma Phys. 44 (2004) 57.
[18] VMECwiki.
[19] Neu, et al., Fusion Eng. Des. 8 (2017) 124.
[20] Semenova, Fe-Ni-W. Landolt-Börnstein Group IV Physical Chemistry, (2009) 11D5.
[21] Alam et al., Fusion materials semiannual progress report DOE-ER-0313/65, 2018.
[22] You, et al., J. Nucl. Mater. 299 (1) (2001).
[23] Wallis et al. (2019), Materials Science & Eng. A 744.
[24] Klecka, et al., Nucl. Mater. Energy 8 (2023) 34.
[25] Mayer, et al., Phys. Scripta (2021) 96.
[26] Grammes, et al., Fusion Eng. Design 9 (2023) 188.